The Synthesis, Structural and Spectroscopic Studies of $[Ru_2Rh_2H_2(CO)_{12}]$‡

Jouni Pursiainen and Tapani A. Pakkanen*
Department of Chemistry, University of Joensuu, SF-80101 Joensuu 10, Finland
Brian T. Heaton*,† and Claudio Seregni
Chemical Laboratory, The University of Kent, Canterbury CT2 7NH
Robin G. Goodfellow
Department of Inorganic Chemistry, The University, Bristol BS8 1TS

The synthesis of $[Ru_2Rh_2H_2(CO)_{12}]$ is reported, together with *X*-ray structural and multinuclear, variable-temperature n.m.r. studies. The structure, both in the solid state and at low temperature in solution, is related to that of $[Rh_4(CO)_{12}]$ with one basal rhodium and the apical rhodium atoms being replaced by ruthenium atoms; the hydrogen atoms are both bonded to the apical ruthenium and bridge Ru–Ru and Ru–Rh edges of the Ru_2Rh_2 tetrahedron. At higher temperatures, both hydrogen and carbonyl fluxionality is observed.

Much work has been done on bimetallic iron–cobalt and ruthenium–cobalt cluster compounds.[1] However, there are not many reports of related compounds between the heavier elements of the iron and cobalt groups.[1–5] We now report a new synthetic route for $[Ru_2Rh_2H_2(CO)_{12}]$ and the characterisation of this compound by *X*-ray crystallography and variable-temperature n.m.r. spectroscopy (^1H, ^1H-{^{103}Rh}, ^{13}C, ^{13}C-{^1H}, and ^{13}C-{^{103}Rh}). A preliminary report of the structural work has already appeared.[2]

Results and Discussion

Synthesis.—The main problem in the synthesis of ruthenium–rhodium mixed-metal clusters is to find stable but reactive species of either metal. In this work $[Rh(CO)_4]^-$ has been used since, unlike $[Ru(CO)_4]^{2-}$, it is thermally stable at room temperature in tetrahydrofuran (thf) solution. Unfortunately, the readily isolable salt $[N(PPh_3)_2][Rh(CO)_4]$ cannot be used since, as found for $[N(PPh_3)_2][CoRu_3(CO)_{13}]$,[6] the formation of a neutral hydride cluster is prevented by the presence of the large cation. Therefore, in our earlier report, $Na[Rh(CO)_4]$ was synthesised by the reduction of $[Rh_2(CO)_4Cl_2]$ by metallic sodium and the thf filtrate was then used immediately.[2,7] It is, however, more advantageous to prepare the rhodate salt in KOH–dimethyl sulphoxide (dmso) media from $RhCl_3 \cdot 3H_2O$.[8] In this work $[Rh(CO)_4]^-$ was extracted with thf from the KOH–dmso solution and was then used immediately for the synthesis of $[Ru_2Rh_2H_2(CO)_{12}]$. Reaction of $[Rh(CO)_4]^-$ with $[Ru_3(CO)_{12}]$ yields an unstable reddish anion, which has not yet been characterised. The anion is treated with H_3PO_4 to obtain $[Ru_2Rh_2H_2(CO)_{12}]$, which is extracted from the acid phase with hexane. Additional extraction with CH_2Cl_2 also yields $[RuRh_5(CO)_{16}]^-$.[9] The i.r. spectrum of $[Ru_2Rh_2H_2(CO)_{12}]$ shows bands at 2 108vw, 2 084vs, 2 064vs, 2 056vs, 2 044w, 2 034s, 2 021m, 2 012m, 1 913m, and 1 860m cm^{-1}.

It is surprising that the reaction of $Na[Co(CO)_4]$ with $[Ru_3(CO)_{12}]$, using quite similar conditions, yields only $[Ru_3CoH(CO)_{13}]$.[6] We have so far been unable to obtain any evidence for $[Ru_3RhH(CO)_{13}]$. However, $[Ru_3RhH(CO)_{13}]$ might be expected to be less stable because of the presence of 13 carbonyls around the metal tetrahedron. Two related hydride clusters, $[Os_2Co_2H_2(CO)_{12}]$[10] and $[Ru_2Co_2H_2(CO)_{12}]$,[11] have been reported previously.

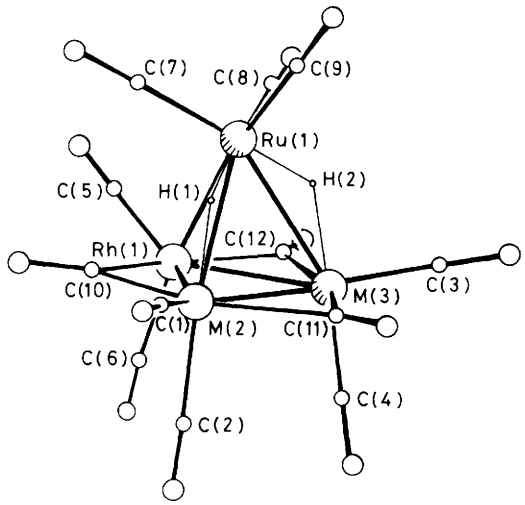

Figure 1. The schematic representation and numbering scheme of $[Ru_2Rh_2H_2(CO)_{12}]$

X-*Ray Crystallography.*—The molecular structure of $[Ru_2Rh_2H_2(CO)_{12}]$ is shown in Figure 1. The Ru_2Rh_2 stoicheiometry is consistent with *X*-ray fluorescence, multinuclear n.m.r. and *X*-ray diffraction measurements. The hydrogen atoms bridge a Ru–Rh and a Ru–Ru bond [designated Ru(1)–M(2) and Ru(1)–M(3) respectively in the *X*-ray work]. A bridging hydrogen lengthens a metal–metal bond and has a repulsive effect on the carbonyl groups.[12] Thus, from the crystallographic determination, the hydrogen positions can be inferred from the data in Tables 1 and 2. Hydrogen prefers to bridge the Ru–Ru bond in $[Ru_2Rh_2H_2(CO)_{12}]$ as found previously in $[Ru_2Co_2H_2(CO)_{12}]$.[11] The other hydrogen atom, however, occupies a different position to that found in $[Ru_2Co_2H_2(CO)_{12}]$, where a $RuCo_2$ face between the axial carbonyls is occupied. In $[Ru_2Co_2H_2(CO)_{12}]$, the Ru(1)–Ru(2)–$CO_{eq.}$ angle is 111.2°, which is consistent with the presence of a bridging hydrogen on the Ru–Ru edge, whereas the Ru(1)–Co–$CO_{eq.}$ angles are as low

† *Present address*: Donnan Laboratories, The University, Liverpool L69 3BX.

‡ 1,2;1,4;2,4-Tri-μ-carbonyl-1,1,2,2,3,3,3,4,4-nonacarbonyl-1,3;3,4-di-μ-hydrido-*tetrahedro*-dirhodiumdiruthenium.

Supplementary data available (No. SUP 56440, 3 pp.): thermal parameters. See Instructions for Authors, *J. Chem. Soc., Dalton Trans.*, 1986, Issue 1, pp. xvii—xx. Structure factors are available from the editorial office.

Table 1. Bond lengths (Å) with estimated standard deviations in parentheses

Rh(1)–Ru(1)	2.730(1)	M(3)–C(3)	1.912(4)	M(2)–C(10)	2.119(5)	O(4)–C(4)	1.126(6)
Rh(1)–M(2)	2.760(1)	M(3)–C(4)	1.887(5)	M(2)–C(11)	2.132(5)	O(5)–C(5)	1.113(7)
Rh(1)–M(3)	2.744(1)	Rh(1)–C(5)	1.884(5)	M(3)–C(11)	2.216(5)	O(6)–C(6)	1.124(6)
Ru(1)–M(2)	2.889(1)	Rh(1)–C(6)	1.948(5)	Rh(1)–C(12)	2.131(5)	O(7)–C(7)	1.140(6)
Ru(1)–M(3)	2.920(1)	Ru(1)–C(7)	1.905(4)	M(3)–C(12)	2.111(5)	O(8)–C(8)	1.121(6)
M(2)–M(3)	2.782(1)	Ru(1)–C(8)	1.917(5)	O(1)–C(1)	1.136(7)	O(9)–C(9)	1.114(5)
M(2)–C(1)	1.903(5)	Ru(1)–C(9)	1.931(4)	O(2)–C(2)	1.120(7)	O(10)–C(10)	1.134(6)
M(2)–C(2)	1.895(5)	Rh(1)–C(10)	2.126(5)	O(3)–C(3)	1.137(5)	O(11)–C(11)	1.124(6)
						O(12)–C(12)	1.147(6)

Table 2. Bond angles (°)*

Ru(1)–Rh(1)–M(2)	63.5	M(2)–Rh(1)–C(12)	110.1(1)	Rh(1)–M(2)–C(10)	49.6(1)	Ru(1)–M(3)–C(12)	79.3(1)
Ru(1)–Rh(1)–M(3)	64.5	M(3)–Rh(1)–C(12)	49.4(1)	Ru(1)–M(2)–C(10)	79.2(1)	M(2)–M(3)–C(12)	109.8(1)
M(2)–Rh(1)–M(3)	60.7	C(5)–Rh(1)–C(12)	96.2(2)	M(3)–M(2)–C(10)	108.9(1)	C(3)–M(3)–C(12)	102.8(2)
Rh(1)–Ru(1)–M(2)	58.7	C(6)–Rh(1)–C(12)	96.8(2)	C(1)–M(2)–C(10)	98.4(2)	C(4)–M(3)–C(12)	93.1(2)
Rh(1)–Ru(1)–M(3)	58.0	C(10)–Rh(1)–C(12)	159.1(2)	C(2)–M(2)–C(10)	98.4(2)	C(11)–M(3)–C(12)	158.3(2)
M(2)–Ru(1)–M(3)	57.2	Rh(1)–Ru(1)–C(7)	92.3(1)	Rh(1)–M(2)–C(11)	110.9(1)	M(2)–C(1)–O(1)	179.1(5)
Rh(1)–M(2)–Ru(1)	57.7	M(2)–Ru(1)–C(7)	95.9(1)	Ru(1)–M(2)–C(11)	87.0(1)	M(2)–C(2)–O(2)	179.5(5)
Rh(1)–M(2)–M(3)	59.4	M(3)–Ru(1)–C(7)	146.7(1)	M(3)–M(2)–C(11)	51.6(1)	M(3)–C(3)–O(3)	177.8(5)
Ru(1)–M(2)–M(3)	61.9	M(2)–Ru(1)–C(8)	149.7(1)	C(1)–M(2)–C(11)	99.7(2)	M(3)–C(4)–O(4)	179.3(3)
Rh(1)–M(3)–Ru(1)	57.5	Rh(1)–Ru(1)–C(8)	92.1(1)	C(2)–M(2)–C(11)	94.6(2)	Rh(1)–C(5)–O(5)	177.9(5)
Rh(1)–M(3)–M(2)	59.9	M(3)–Ru(1)–C(8)	102.0(1)	C(10)–M(2)–C(11)	160.2(2)	Rh(1)–C(6)–O(6)	176.9(5)
Ru(1)–M(3)–M(2)	60.8	C(7)–Ru(1)–C(8)	93.2(2)	Rh(1)–M(3)–C(3)	151.5(1)	Ru(1)–C(7)–O(7)	177.0(4)
Ru(1)–Rh(1)–C(5)	91.5(1)	Rh(1)–Ru(1)–C(9)	169.8(2)	Ru(1)–M(3)–C(3)	115.8(1)	Ru(1)–C(8)–O(8)	179.0(4)
M(2)–Rh(1)–C(5)	140.2(2)	M(2)–Ru(1)–C(9)	113.0(2)	M(2)–M(3)–C(3)	145.2(1)	Ru(1)–C(9)–O(9)	179.1(5)
M(3)–Rh(1)–C(5)	137.7(2)	M(3)–Ru(1)–C(9)	113.1(1)	Rh(1)–M(3)–C(4)	96.9(1)	Rh(1)–C(10)–M(2)	81.1(2)
Ru(1)–Rh(1)–C(6)	170.3(1)	C(7)–Ru(1)–C(9)	94.7(2)	Ru(1)–M(3)–C(4)	151.8(1)	Rh(1)–C(10)–O(10)	138.6(4)
M(2)–Rh(1)–C(6)	107.5(1)	C(8)–Ru(1)–C(9)	94.8(2)	M(2)–M(3)–C(4)	97.6(1)	M(2)–C(10)–O(10)	140.3(4)
M(3)–Rh(1)–C(6)	108.5(1)	Rh(1)–M(2)–C(1)	145.7(2)	C(3)–M(3)–C(4)	92.2(2)	M(2)–C(11)–M(3)	79.5(2)
C(5)–Rh(1)–C(6)	98.1(2)	Ru(1)–M(2)–C(1)	110.7(2)	Rh(1)–M(3)–C(11)	108.8(1)	M(2)–C(11)–O(11)	141.7(4)
Ru(1)–Rh(1)–C(10)	82.9(1)	M(3)–M(2)–C(1)	148.9(1)	Ru(1)–M(3)–C(11)	84.7(1)	M(3)–C(11)–O(11)	138.6(4)
M(2)–Rh(1)–C(10)	49.3(1)	Rh(1)–M(2)–C(2)	100.2(1)	M(2)–M(3)–C(11)	48.9(1)	Rh(1)–C(12)–M(3)	80.6(2)
M(3)–Rh(1)–C(10)	110.1(1)	Ru(1)–M(2)–C(2)	156.4(1)	C(3)–M(3)–C(11)	97.3(2)	Rh(1)–C(12)–O(12)	138.6(4)
C(5)–Rh(1)–C(10)	100.0(2)	M(3)–M(2)–C(2)	101.0(1)	C(4)–M(3)–C(11)	94.2(2)	M(3)–C(12)–O(12)	140.7(4)
Ru(1)–Rh(1)–C(12)	83.6(1)	C(1)–M(2)–C(2)	92.3(2)	Rh(1)–M(3)–C(12)	50.0(1)		

* E.s.d.s. have been rounded to one decimal place and, where not given, are less than 0.05°.

as 80.8 and 75.2°. The average values for M–M′–$CO_{ax.}$ angles [M,M′ ≠ Ru(1)] are 102.0° for $[Ru_2Rh_2H_2(CO)_{12}]$ and 114.5° for $[Ru_2Co_2H_2(CO)_{12}]$. Difference Fourier maps were used to assign the metal atoms. The maps were approximately identical when all the metal atoms were treated as ruthenium or as rhodium [Figure 2, Table 3(*a*) and (*b*)] giving no clear help with the metal assignment. Various combinations of two ruthenium and rhodium atoms were then refined leading to the final assignment, which is entirely in agreement with the structure deduced from low-temperature n.m.r. studies (see below). The metal atom A can be assigned as ruthenium and metal atom D as rhodium [Figure 3, Table 3(*c*) and (*d*)], but no difference could be seen between metal atoms B and C. They behaved like average values of the two metals and the refinement of these metal atoms as 50%:50% Ru:Rh produced featureless difference maps (Figure 4). The site occupation factor of rhodium refined to 48.7% for metal atom B and to 53.6% for metal atom C indicating an average occupancy by these two atoms. Final refinement with 2 973 intensities [$I \geqslant 2.5\sigma(I)$] converged to $R = 0.0215$ and $R' = 0.0249$ [$w = 1/(\sigma^2|F| + 0.005F^2)$]. An attempt to resolve the disorder by refining the structure as space group *P*1 led to lower R values and featureless difference Fourier maps only for the non-centrosymmetric arrangement. However, the final structure of the cluster was not satisfactory due to the low reflection/-parameter ratio. The molecule contains four different Ru–Rh bond distances of which unfortunately only Ru(1)–Rh(1) and

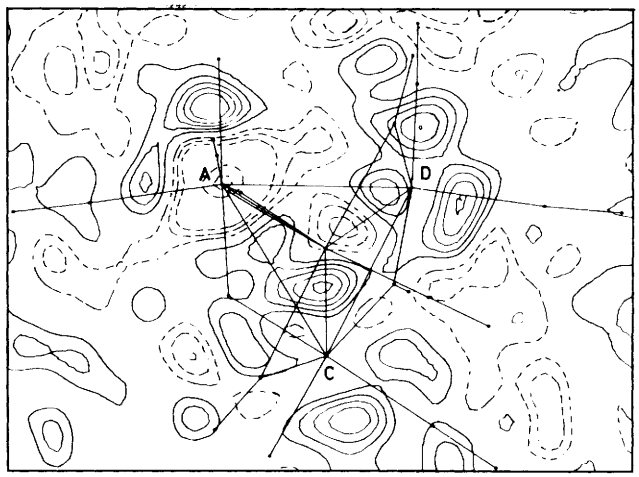

Figure 2. Difference Fourier map of the plane containing metal atoms A, C, and D, when all the metal atoms are treated as rhodium [Table 3 (*a*)]

M(2)–M(3) can be identified. These distances lie between the Rh–Rh bond length in $[Rh_4(CO)_{12}]$ (mean value 2.73 Å)[13] and the Ru–Ru bond lengths in $[Ru_4H_4(CO)_{12}]$ (mean values: hydrogen-bridged, 2.95 Å; non-bridged, 2.79 Å).[14]

The Ru(1)–Rh(1) bond is shorter than the non-bridged

Table 3. Behaviour of the metal positions in difference Fourier maps (Figures 2—4)*

	Metal atom				
	A	B	C	D	*R*
(*a*)	Rh(−I)	Rh(—)	Rh(—)	Rh(I)	0.0269
(*b*)	Ru(−I)	Ru(—)	Ru(—)	Ru(I)	0.0266
(*c*)	Ru(—)	Rh(−I)	Rh(−I)	Ru(II)	0.0280
(*d*)	Rh(−II)	Ru(I)	Ru(I)	Rh(—)	0.0286
(*e*)	Ru(—)	50% (—)	50% (—)	Rh(—)	0.0258

* Relative intensities: no peak (—); a low peak (I); a high peak, (II). A negative value represents negative electron density. Metal atom A was assigned as Ru(1) and metal atom D as Rh(1).

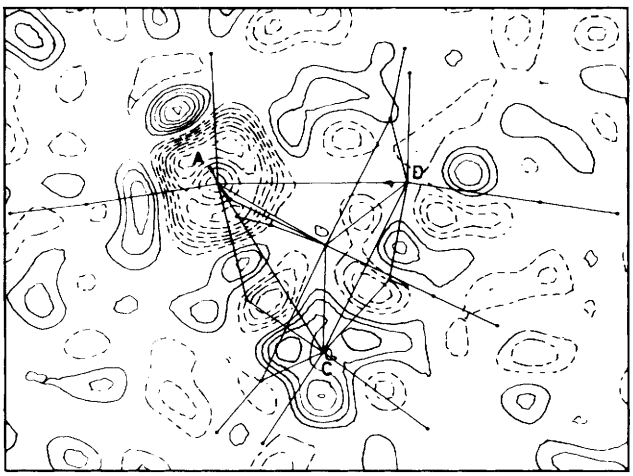

Figure 3. Difference Fourier map of the plane containing metal atoms A, C, and D, when metal atoms A and D are treated as rhodium and B and C as ruthenium [Table 3(*d*)]

Ru–Rh bonds in $[Ru_3Rh_2(CO)_{13}(PEt_3)(\mu_4\text{-}PPh)]$ (2.783 and 2.758 Å).[3] The non-bridged (2.962 Å) and carbonyl-bridged (2.998 and 3.005 Å) Ru–Rh bonds in the pentanuclear $[RuRh_4(CO)_{15}]^{2-}$ anion[4] are longer than any of the bonds in $[Ru_2Rh_2H_2(CO)_{12}]$.

Variable-temperature Multinuclear N.M.R. Studies.—The low-temperature ^1H n.m.r. spectrum of $[Ru_2Rh_2H_2(CO)_{12}]$ [Figure 5(*a*)] is fully consistent with the solid-state structure [Figure 1; M(2) = Rh^2, M(3) = Ru^2] and variable-temperature ^1H n.m.r. spectra [Figure 5(*b*)—(*e*)] reveal some interesting H-exchange processes. At −30 °C, there are two equally intense resonances due to H^1 and H^2 [$\delta(H^1) = -19.2$, $^1J(Rh^2\text{–}H^1) = 17.0$; $\delta(H^2) = -21.3$ p.p.m.; $^3J(H^1\text{–}H^2) = 2.0$ Hz] and ^1H-$\{^{103}Rh\}$ INDOR measurements allow the chemical shift of Rh^2 to be obtained [$\delta(Rh^2) = -265$ p.p.m.]. On decoupling at the frequency corresponding to Rh^2, both resonances become doublets due to the residual coupling, $^3J(H^1\text{–}H^2)$, whereas decoupling at the Rh^1 frequency (see below), has little effect on either resonance. On raising the temperature, the resonance due to H^1 becomes a well resolved triplet due to rapid H-exchange between the two Ru_{apical}–Rh edges [time-averaged $J(Rh^{1,2}\text{–}H^1) = 8.5$ Hz], with the resonance due to H^2 remaining unchanged. ^1H-$\{^{103}Rh\}$ INDOR spectra at 4 °C clearly show two well resolved peaks at −270 and −637 p.p.m. due to Rh^2 and Rh^1 respectively. At higher temperatures, both ^1H resonances broaden due to the onset of RhHRu ⟷ RuHRu exchange. Rationalisation of this difference in activation

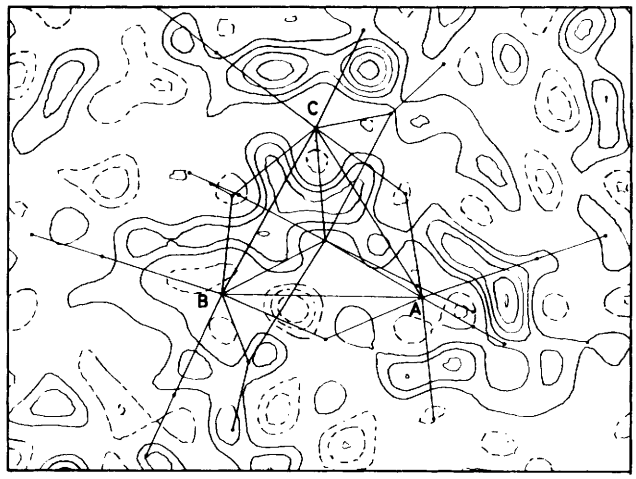

Figure 4. Difference Fourier map of the plane containing metal atoms A, B, and C, when metal atom A is treated as ruthenium, metal atom D as rhodium, and metal atoms B and C are 50% occupied by ruthenium and rhodium [Table 3(*e*)]

energies for H-mobility undoubtedly stems from the preference of both ruthenium atoms to maintain an 18-electron configuration. The initial movement of H^1 between the Ru^1–Rh^2 and Ru^1–Rh^1 edges does not affect this whereas migration of H^2 away from the Ru^1–Ru^2 edge without simultaneous replacement by H^1 leaves Ru^2 electron deficient and this process would therefore be expected to be of higher energy.

The 50-MHz ^{13}C-$\{^1H\}$ n.m.r. spectrum at −47 °C [Figure 6(*a*)] is also entirely consistent with the solid-state structure [Figure 1; M(2) = Rh^2, M(3) = Ru^2] in which all 12 carbonyls are inequivalent. Of the nine resonances due to the terminal carbonyls, besides the expected rhodium coupling to four carbonyls (CO^1, CO^2, CO^5 and CO^6), there is clearly H–CO coupling to the resonances at 178.4, 189.1, and 190.1 p.p.m. These have been assigned to CO^2, CO^7, and CO^8 respectively by means of specific H-decoupling experiments [Figure 6(*b*)—(*d*)]. Coupling to the fourth carbonyl *trans* to the hydrides, $^2J(H^2\text{–}CO^4)$, is only observed at higher fields and lower temperatures because the values of $\delta(CO^3)$ and $\delta(CO^4)$ are coincident. Variable-temperature measurements show that carbonyl exchange first involves coalescence of resonances at 178.4 (CO^2), half of the doublet at 184.3, and the doublet of doublets at 222.9 p.p.m. (CO^{10}) and, as a result, half of the resonance at 184.3 p.p.m. must be due to CO^1. Thus, the lowest energy carbonyl-exchange process in $[Ru_2Rh_2H_2(CO)_{12}]$ involves conversion of the bridging carbonyl (CO^{10}) to a terminal carbonyl on Rh^2 followed by a localised rotation involving CO^1, CO^2, and CO^{10} about Rh^2. The other half of the doublet at 184.3 p.p.m. is thus due to the other radial carbonyl on rhodium, CO^5. These assignments of the carbonyl resonances due to the carbonyls associated with the rhodium atoms were confirmed by ^{13}C-$\{^{103}Rh\}$ measurements and, by analogy with this and previous work,[15] it seems reasonable to assign the three apical Ru carbonyls (CO^7, CO^8, and CO^9) to the resonances at 189.1, 190.1, and 192.3 p.p.m. respectively. All these data are summarised in Table 4.

Unfortunately, because of slow precipitation over prolonged periods at this temperature, it was impossible to carry out selective spin inversion/recovery measurements using the DANTE pulse sequence[16] in order to obtain a more detailed understanding of carbonyl migrations in this cluster. However, at room temperature all the carbonyls are fluxional and give a single broad resonance at 189.5 p.p.m.

Table 4. N.m.r. data for $[Ru_2Rh_2H_2(CO)_{12}]$ in CD_2Cl_2 [see Figure 1; M(2) = Rh^2, M(3) = Ru^2][a]

δ/p.p.m.		J/Hz	
$\delta(H^1)$	−19.2	$^1J(Rh^1–CO^5)$	72.4
$\delta(H^2)$	−21.3	$^1J(Rh^1–CO^6)$	61.4
		$^1J(Rh^2–CO^1)$	72.4
$\delta(CO^1)$	184.3	$^1J(Rh^2–CO^2)$	61.4
$\delta(CO^2)$	178.4	$^1J(Rh^1–CO^{10})$	39.3[b]
$\delta(CO^3)$	186.0[c]	$^1J(Rh^2–CO^{10})$	22.2[b]
$\delta(CO^4)$	186.0[d]	$^1J(Rh^1–CO^{12})$	14.0[e]
$\delta(CO^5)$	184.3	$^1J(Rh^2–CO^{11})$	20.0[e]
$\delta(CO^6)$	175.9		
$\delta(CO^7)$	189.1[d]	$^1J(Rh^2–H^1)$	17.0
$\delta(CO^8)$	190.1		
$\delta(CO^9)$	192.3[c]	$^3J(H^1–H^2)$	2
$\delta(CO^{10})$	222.9		
$\delta(CO^{11})$	226.4[f]	$^2J(H^1–CO^2)$	*ca.* 19
$\delta(CO^{12})$	242.2[f]	$^2J(H^1–CO^8)$	9.5
		$^2J(H^2–CO^4)$	*ca.* 19
$\delta(Rh^1)$	−637	$^2J(H^2–CO^7)$	13.3
$\delta(Rh^2)$	−270		

[a] Hydrogen-1, ^{13}C, and ^{103}Rh n.m.r. data at −30, −47, and +4 °C respectively; ^1H and ^{13}C chemical shifts are from $SiMe_4$ and $\delta(^{103}Rh)$ = 0 p.p.m. at 3.16 MHz at a magnetic field such that the protons in $SiMe_4$ resonate at exactly 100 MHz. [b,c,d,e,f] Within each pair, the assignments could be interchanged, but see text.

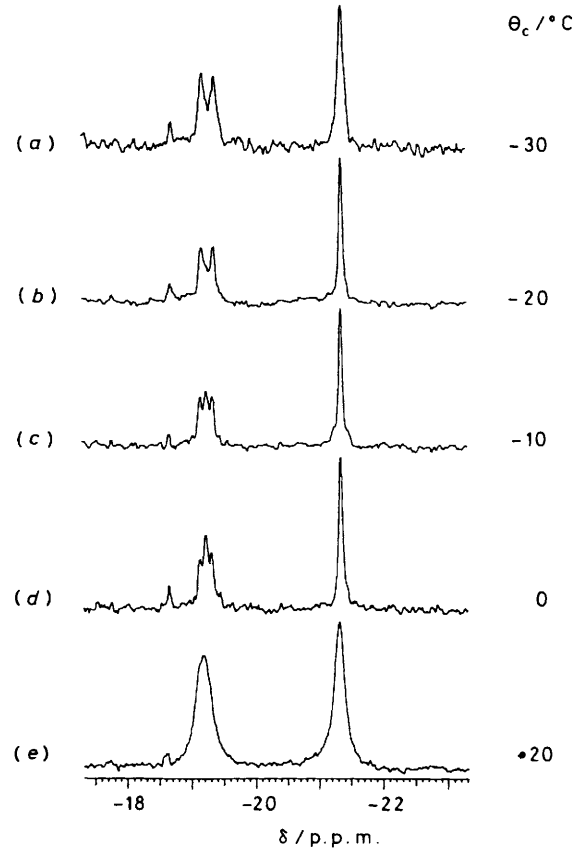

Figure 5. Variable-temperature 90-MHz ^1H n.m.r. spectrum of $[Ru_2Rh_2H_2(CO)_{12}]$ in CD_2Cl_2: labelling as in Figure 1 [M(2) = Rh^2, M(3) = Ru^2]

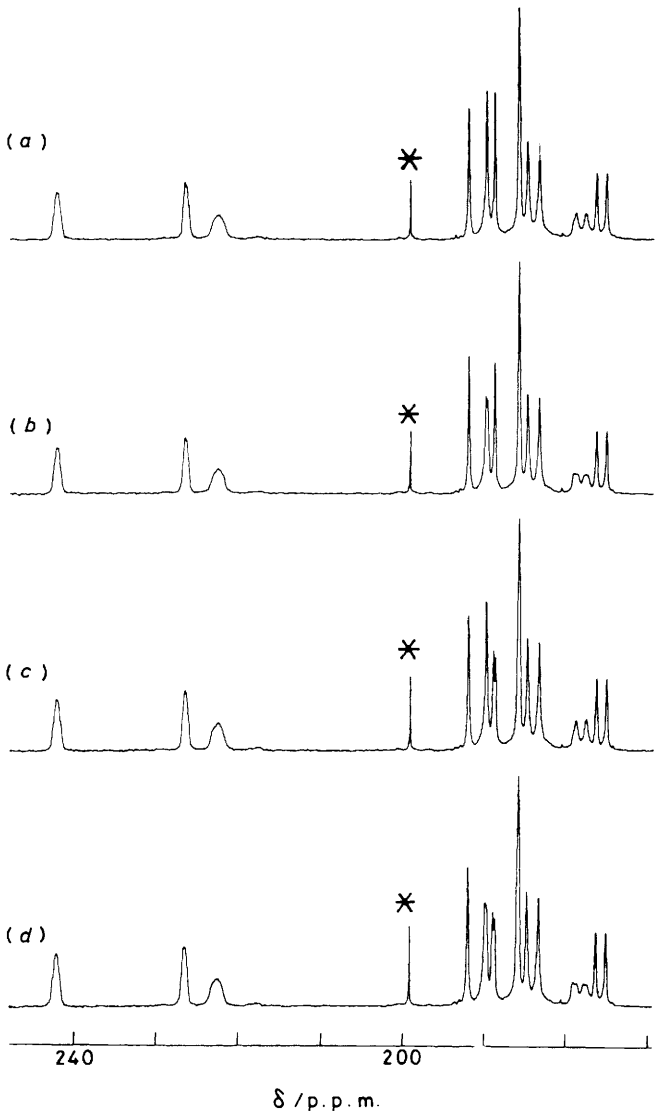

Figure 6. 50.3-MHz ^{13}C n.m.r. spectra of $[Ru_2Rh_2H_2(CO)_{12}]$ at −47 °C in CD_2Cl_2; labelling as in Figure 1 [M(2) = Rh^2, M(3) = Ru^2]. (*a*) $H^{1,2}$-decoupled, (*b*) H^2-decoupled, (*c*) H^1-decoupled, (*d*) non-H-decoupled. * Is an impurity, $[Ru_4H_4(CO)_{12}]$

It is worth noting that, in agreement with our previous suggestions concerning the assignment of the carbonyl resonances in $[Rh_4(CO)_{12}]$,[15] the rhodium axial carbonyl resonances in $[Ru_2Rh_2H_2(CO)_{12}]$ (CO^2 and CO^6) both occur at lower frequency than the two rhodium radial carbonyl resonances (CO^1 and CO^5) and also have $^1J(Rh–CO_{ax.}) < {}^1J(Rh–CO_{rad.})$ with values very similar to those found in $[Rh_4(CO)_{12}]$.

Experimental

All reactions were carried out under a nitrogen atmosphere with deoxygenated solvents. Infrared spectra were recorded on a Perkin-Elmer 297 i.r. spectrophotometer using 0.5-mm NaCl solution cells. Hydrogen-1 and ^1H-{^{103}Rh} INDOR measurements were carried out as described previously[17] at 100 MHz and ^{13}C n.m.r. spectra were obtained on Bruker 200- and 400-MHz spectrometers in 10- and 5-mm n.m.r. tubes, respectively, using a dichloromethane solution containing *ca.* 150 mg of

Table 5. Atom co-ordinates

Atom	*x*	*y*	*z*	Atom	*x*	*y*	*z*
Rh(1)	0.3849(1)	0.3577(1)	0.7752(1)	O(12)	0.5286(4)	0.3353(4)	0.5046(4)
Ru(1)	0.3012(1)	0.0812(1)	0.7487(1)	C(1)	−0.0257(6)	0.1997(5)	0.9283(5)
M(2)	0.1092(1)	0.2719(1)	0.8091(1)	C(2)	0.0419(5)	0.4426(5)	0.8158(5)
M(3)	0.2194(1)	0.2616(1)	0.5553(1)	C(3)	0.1929(5)	0.1830(5)	0.3746(4)
O(1)	−0.1051(5)	0.1569(5)	1.0009(5)	C(4)	0.1815(5)	0.4338(4)	0.5085(4)
O(2)	0.0011(5)	0.5430(4)	0.8194(5)	C(5)	0.5580(5)	0.3337(5)	0.8446(6)
O(3)	0.1728(5)	0.1358(4)	0.2677(3)	C(6)	0.4124(5)	0.5575(5)	0.7865(5)
O(4)	0.1579(4)	0.5359(3)	0.4797(4)	C(7)	0.3504(5)	0.0628(5)	0.9300(4)
O(5)	0.6601(5)	0.3160(5)	0.8829(6)	C(8)	0.4762(5)	0.0455(5)	0.6845(5)
O(6)	0.4301(5)	0.6728(4)	0.7988(5)	C(9)	0.2131(5)	−0.1062(4)	0.7149(4)
O(7)	0.3748(4)	0.0539(4)	1.0401(4)	C(10)	0.2686(5)	0.3470(5)	0.9518(5)
O(8)	0.5776(4)	0.0229(5)	0.6460(4)	C(11)	0.0085(5)	0.1960(4)	0.6226(5)
O(9)	0.1635(5)	−0.2149(4)	0.6965(4)	C(12)	0.4334(5)	0.3267(5)	0.5696(5)
O(10)	0.2859(4)	0.3683(4)	1.0640(3)	H(1)	0.244(7)	0.131(6)	0.631(7)
O(11)	−0.0931(4)	0.1438(4)	0.5788(4)	H(2)	0.148(8)	0.103(7)	0.808(8)

Table 6. Intensities of the hydrogen peaks with different sinθ/λ limitations†

sinθ/λ	$I(H^1)$	$I(H^2)$	$I(*)$
1	89(1)	73(5)	81(2)
0.35	330(1)	240(2)	129(4)
0.30	380(1)	282(2)	141(3)

† The values in parentheses refer to the order of peaks according to descending intensity. $I(*)$ represents the highest peak other than the hydrogen atoms.

sample, which was enriched with ^{13}CO (*ca.* 25%) by direct exchange using standard vacuum-line techniques.

Literature methods were used to synthesise $[Rh(CO)_4]^-$.[7,8] Other chemicals were used as purchased from commercial sources.

Preparation of $[Ru_2Rh_2H_2(CO)_{12}]$.—$[Rh(CO)_4]^-$ was extracted with thf from the KOH–dmso media of the $[Rh(CO)_4]^-$ synthesis (initially 200 mg $RhCl_3 \cdot 3H_2O$) and the extracts were immediately added to a thf solution of $[Ru_3(CO)_{12}]$ (450 mg). The solution was stirred at *ca.* 50 °C for 1 h, during which time it turned a deep reddish brown. The anionic product was precipitated from thf by addition of hexane. The solution was then removed and the solid residue was then treated with 85% H_3PO_4 (2 cm^3). The impure product was extracted into hexane and chromatographed on silica gel. A broad yellow band consisting of $[Ru_3(CO)_{12}]$ and tetranuclear ruthenium hydride clusters was eluted first by hexane followed by a reddish band of the title compound; 52% of the original rhodium was recovered as $[Ru_2Rh_2H_2(CO)_{12}]$ (150 mg).

Crystal Data.—$C_{12}H_2O_{12}Rh_2Ru_2$, M = 746.1, triclinic, space group $P\bar{1}$, a = 9.841(4), b = 9.883(4), c = 10.033(3) Å, α = 94.70, β = 90.84, γ = 98.13(3)°, U = 962.2(6) Å^3, Z = 2, D_c = 2.57 g cm^{-3}, $F(000)$ = 7 219, $\lambda(Mo\text{-}K_\alpha)$ = 0.710 69 Å, $\mu(Mo\text{-}K_\alpha)$ = 32.0 cm^{-1}.

Atom co-ordinates are given in Table 5.

Intensity Measurements.—Air-stable red crystals were grown by slow evaporation of a saturated CH_2Cl_2–hexane (1:1) solution. The data were collected on a Nicolet *R3m* diffractometer. Accurate cell parameters were obtained from 22 centred reflections in the range $25 \leqslant 2\theta \leqslant 30°$. 3 389 Unique reflections were collected within $5 \leqslant 2\theta \leqslant 50°$ by standard procedures. Intensities were corrected for background, polarisation and Lorentz factors. Empirical absorption correction was made from ψ-scan data. The positions of the metal atoms (treated as Ru) and carbonyls were solved by the direct methods of the SHELXTL program packing.[18] These were anisotropically refined to R = 0.0268. To locate the hydrogen atoms a series of difference Fourier maps based on low-angle reflection data were calculated with sinθ/λ limits exchanged relatively to the others (Table 6) and were thus assigned.[19]

X-*Ray Fluorescence.*—A semi-quantitative elemental analysis was made for ruthenium and rhodium using an energy-dispersive electron microprobe analyser using emitted *L*-*X*-ray lines. An approximately 1:1 Ru:Rh ratio could be seen, which together with the known tetranuclear structure fixed the 2:2 stoicheiometry of the cluster core.

Acknowledgements

The Neste Oy Foundation is acknowledged for financial support and the S.E.R.C. for the award of a post-doctoral fellowship (to C. S.) and for high-field n.m.r. facilities. We also thank Dr. B. E. Mann for recording the high-field ^{13}C n.m.r. spectra and Dr. Juhani Jääskeläinen for the *X*-ray fluorescence analysis.

References

1 D. A. Roberts and G. L. Geoffrey, 'Comprehensive Organometallic Chemistry,' Pergamon, Oxford, 1982, vol. 6, p. 763.
2 J. Pursiainen and Tapani A. Pakkanen, *J. Chem. Soc., Chem. Commun.*, 1984, 252.
3 M. J. Mays, P. R. Raithby, and P. L. Taylor, *J. Organomet. Chem.*, 1983, **224**, 252.
4 A. Fuagalli and G. Ciani, *J. Organomet. Chem.*, 1984, **272**, 91.
5 J. F. Knifton, *J. Chem. Soc., Chem. Commun.*, 1983, 729.
6 P. C. Steinhardt, W. L. Gladfelter, A. D. Harley, J. R. Fox, and G. L. Geoffroy, *Inorg. Chem.*, 1980, **19**, 339.
7 P. Chini and S. Martinengo, *Inorg. Chim. Acta*, 1969, **3**, 21.
8 L. Garlaschelli, P. Chini, and S. Martinengo, *Gazz. Chim. Ital.*, 1982, **112**, 285.
9 J. Pursiainen and T. A. Pakkanen, unpublished work.
10 J. R. Moss and W. A. G. Graham, *J. Organomet. Chem.*, 1970, **23**, C23.
11 E. Roland and H. Vahrenkamp, *Organometallics*, 1983, **2**, 183.
12 M. R. Churchill, *Adv. Chem. Ser.*, 1978, **167**, 36.
13 C. H. Wei, *Inorg. Chem.*, 1969, **8**, 2384.

14 R. D. Wilson, S. M. Wu, R. A. Love, and R. Bau, *Inorg. Chem.*, 1978, **17**, 1271.
15 B. T. Heaton, L. Strona, R. Della Pergola, L. Garlaschelli, U. Sartorelli, and I. H. Sadler, *J. Chem. Soc., Dalton Trans.*, 1983, 173.
16 G. A. Morris and R. C. Freeman, *J. Magn. Reson.*, 1978, **29**, 433.
17 P. L. Goggin, R. J. Goodfellow, J. R. Knight, M. G. Norton, and B. F. Taylor, *J. Chem. Soc., Dalton Trans.*, 1973, 2220.
18 G. M. Sheldrick, The SHELXTL System, Revision 2.5, Nicolet Co., Madison, Wisconsin, 1980.
19 S. J. La Placa and J. A. Ibers, *J. Am. Chem. Soc.*, 1963, **85**, 3501.

Received 4th June 1985; *Paper* 5/947